3,11,19-Trithia[3.3.3]pyridinophane: Structural Diversity in Its Transition Metal Complexes

Muthalagu Vetrichelvan,[a] Yee-Hing Lai,*[a] and Kum Fun Mok[a]

Keywords: Coordination polymers / Macrocycles / Structural diversity / Transition metals / Zwitterions

The pyridine-containing aza-thia macrocycle 3,11,19-trithia[3.3.3]pyridinophane (**10**) and its complexes with Ni^{II}, Pd^{II}, Cu^{I}, Ag^{I} and Hg^{II} were synthesised and their crystal structures were determined. The Ni^{II} and Hg^{II} complexes (**11**, **12**) are mononuclear with **10** serving as an unusual quinquedentate ligand. The Cu^{I} complex **13** is also mononuclear with **10** being tetra-coordinated to a tetrahedral Cu^{I}. Palladium(II) forms a binuclear complex **14** which exists as an inorganic zwitterion and both Pd^{II} metal ions adopt the expected square-planar geometry with facial coordination. Silver(I) forms one-dimensional coordination polymers (**15** and **16**) with **10** and these exhibit two different coordination modes, namely tetrahedral and trigonal planar. It was found that the macrocycle **10** did not show any selectivity among a series of metal ions. The electronic and redox properties of several complexes were studied.

Introduction

Crystal engineering remains one of the most fascinating areas of research in modern inorganic chemistry. It has given rise to many remarkable structures by using transition metals through the development of coordination polymers, the construction of molecular architectures and the self-assembly of complex molecular structures.[1−12] The coordination chemistry of pyridine-containing macrocycles is of particular interest due to the effective coordination ability of pyridine.[13] Parallel to this, binuclear macrocyclic complexes have also attracted much attention as catalysts and models for certain metalloenzymes.[14,15] There is also a need to understand the nature and extent of metal-metal interactions. Schröder et al.[16−18] and others[19−22] have reported a series of coordination polymers derived from Ag^{I} and thioether macrocycles **1−5** as well as other functionalised thioether macrocycles.[23,24] The search for appropriate organic building blocks for the construction of coordination polymers and the study of binuclear complexes led us to investigate the ligand **10**. The intramolecular layout of the three pyridine rings in **10** means that it is able to form a cone-like conformation similar to that of calixarenes and thus **10** was expected to exhibit interesting complexation properties.

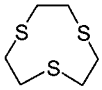

[9]aneS$_3$, **1**

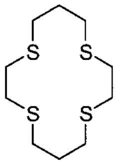

[14]aneS$_4$, **2**

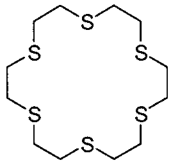

[18]aneS$_6$, **3**

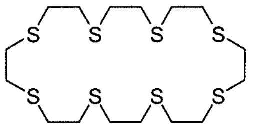

[24]aneS$_8$, **4**

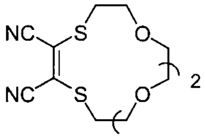

[15]aneS$_2$O$_3$, **5**

We report herein a new synthetic route to the macrocycle **10** and the preparation of a series of its transition metal complexes **11−16**. The solid-state structures of the metal complexes, their electronic and redox properties and an extraction study of the macrocycle are discussed. To the best of our knowledge, complexes **15** and **16** are the first examples of one-dimensional Ag^{I} coordination polymers exhibiting two different coordination geometries with the same macrocyclic ligand. The palladium complex **14** is dinuclear and exists as an inorganic zwitterion while Cu^{I}, Ni^{II} and Hg^{II} form mononuclear complexes **11−13** having different degrees of coordination.

Results and Discussion

Syntheses

The macrocycle **10** was previously isolated as a side-product in a reaction between bis(bromomethyl)pyridine and

---

[a] Department of Chemistry, National University of Singapore,
3 Science Drive 3, Singapore 117543
Fax: (internat.) + 65-6779-1691
E-mail: chmlaiyh@nus.edu.sg

Supporting information for this article is available on the WWW under http://www.eurjic.org or from the author.

DOI: 10.1002/ejic.200300835

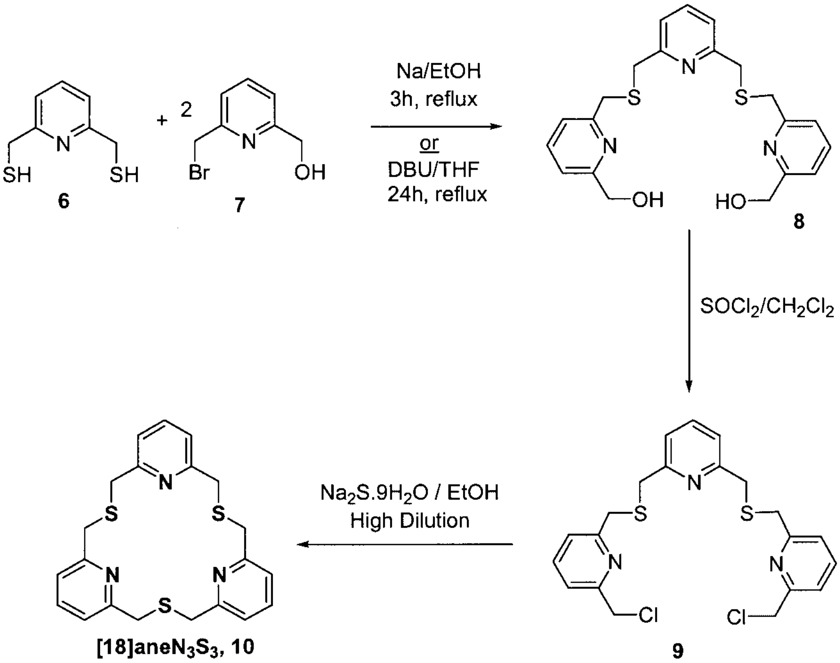

Scheme 1. Synthetic scheme for the preparation of the macrocycle **10**

thioacetamide.[25] An improved synthetic route to **10** was employed in this work starting from known precursors[26] **6** and **7** (Scheme 1) giving a 50% overall yield of **10**. The reaction between **6** and **7** to afford the diol **8** could be achieved in two ways: in the presence of DBU/THF or with Na/ethanol. The latter was found to need a shorter reaction time and gave a higher yield of **8**. Treatment of the diol **8** with thionyl chloride gave the dichloride **9** in a 90% yield. The macrocycle [18]aneN_3S_3 **10** was isolated in a 70% yield via an intramolecular coupling reaction of **9** with sodium sulfide under high-dilution conditions.[27,28]

The metal complexes **11−16** (Figure 1) of the macrocycle **10** were prepared by reactions of the ligand with the appropriate metal salts, respectively; details are given in the Exp. Sect.

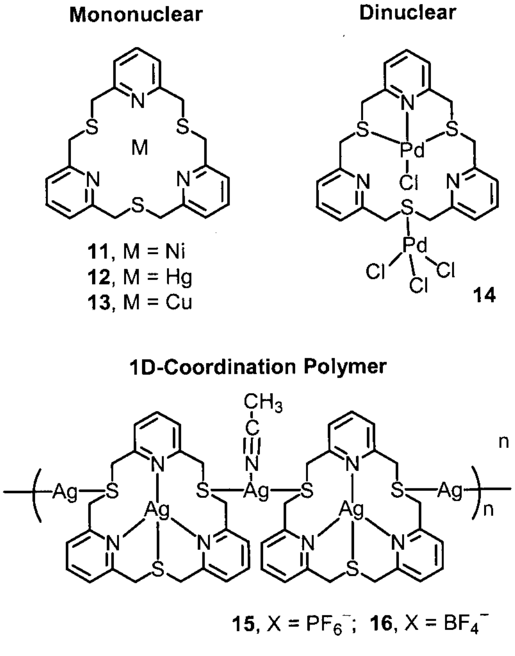

Figure 1. Structural diversity of complexes **11−16**

Structure Description of [Ni(10)(ClO_4)$_2$] (11)

In the crystal structure of the nickel complex **11** (Figure 2), the nickel centre is five-coordinate. Although the macrocycle **10** has six donor atoms, a rare pentacoordinate nickel is observed in this case, which is probably due to a relatively large macrocyclic cavity. The asymmetric unit contains two independent halves of the molecule. The ORTEP diagram of the complex is shown in Figure 2 (left) and selected bond lengths and bond angles are given in Table 1 and Table 2, respectively.

The geometric parameter τ, which is equal to zero for a perfect square pyramid and becomes unity for a perfect trigonal bipyramid,[29] was calculated to be about 0.65, thus indicating that the nickel in complex **11** adopts a distorted trigonal bipyramidal geometry. Three pyridine nitrogens form a trigonal plane and two of the benzylic sulfur atoms occupy the axial positions of the trigonal bipyramids. Pentacoordination is relatively rare for Ni^{II}, which more often forms either high-spin octahedral or low-spin square-planar complexes.[30] In addition, Ni^{II} complexes with pentadentate ligands are often hexacoordinate due to bonding

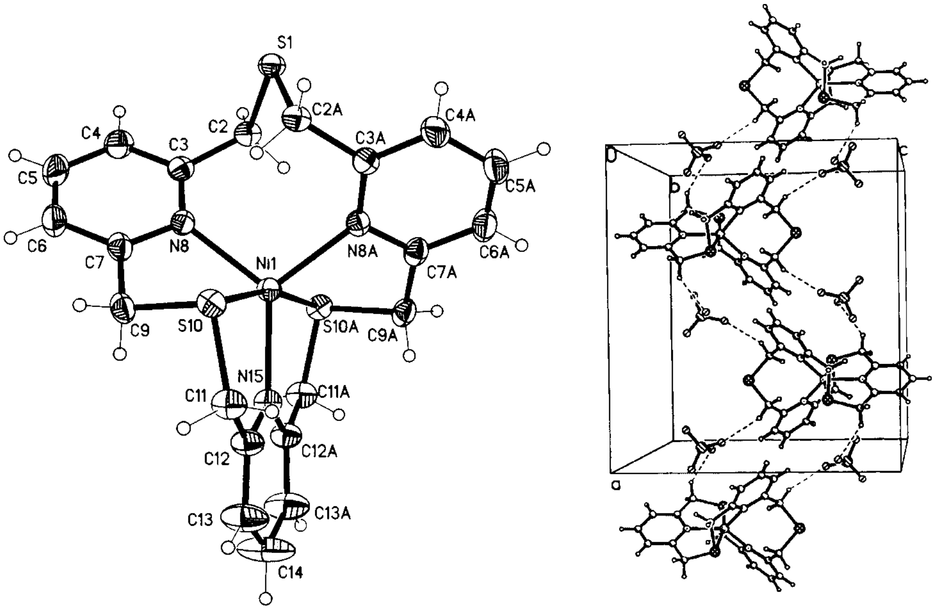

Figure 2. (left) ORTEP drawing of the Ni^{II} complex **11**; (right) packing diagram of complex **11** along the *b*-axis

to a solvent molecule or an anion.[31] A ligand with a 15- or 16-membered ring offers an ideal cavity for a six-coordinate nickel ion. The 18-membered ring in **10** is supposedly sufficiently large for this purpose. In the novel Ni^{II} complex **11**, a pentacoordinate nickel is unusually entrapped by a hexadentate macrocycle. This may be due to unfavourable steric interactions or geometrical strain developed in the ligand if all six donor groups in **11** are bonded to the Ni^{II} ion in an octahedral arrangement.[32] In addition hydrogen bonding may play a role in stabilizing the helical structure of the complex in the crystal packing [Figure 2 (right)] thus discouraging the utilisation of the sixth coordination position of the metal centre. This, we believe, is an unusual type of geometry rarely reported in the literature.

The Ni−N and Ni−S bond lengths in **11** are similar to those reported in the literature.[33] The Ni−N bond lengths are typical of high-spin Ni^{II} complexes with nitrogen donor atoms.[30] The perchlorate anions have the expected tetrahedral geometry although the variation in bond lengths and angles and the large thermal parameters suggest that some degree of disorder is present.

The packing diagram of **11** in the solid state along the *b*-axis is shown in Figure 2 (right). The adjacent molecules are linked through weak intermolecular hydrogen bonding of the type Cl−O···H−C via the benzylic C−H of the pyridine units and the oxygen atom of the perchlorate anions. The adjacent molecules are in an antiparallel array and thereby the overall crystal packing appears as a helix involving two types of hydrogen bonding, with typical bond lengths[34−36] of 2.500Å and 2.473 Å, respectively. Such hydrogen bonding has been found to be important in influencing the nature of the molecular packing in solid-state structures.[37] There is, however, no interaction between two adjacent helices in the crystal packing of **11**.

Structure Description of [$Hg(10)(ClO_4)_2$] (12)

A mononuclear mercury(II) complex of formula $Hg(10)(ClO_4)_2$ is formed when either a 1:2 or a 1:1 ratio of macrocycle **10** and metal salt were used. The X-ray structure of the complex shows that the mercury is coordinated to three pyridine nitrogens and two thioether sulfurs of the macrocycle. The geometric parameter τ for the mercury complex is 0.48, which indicates a distorted square-pyramidal geometry. The ORTEP diagram of the complex is shown in Figure 3 and Table 1 and 2 list the bond lengths and bond angles around the metal ion. One of the thioether sulfurs is not coordinated and it is in an exodentate position even after complexation. Three pyridine nitrogens form a perfect trigonal plane and two of the thioether sulfurs occupy approximately axial positions. The bond angles are very distorted due to two additional interactions of the metal ion with oxygens of the two perchlorate anions. The O···Hg distances are about 3.283 and 3.198 Å, which are too long to be considered as bonding interactions.[38] Due to these weak Hg···O interactions, the mercury ion is pseudo-seven coordinate. The N_{py}−Hg distances in the macrocycle are somewhat shorter than reported earlier.[39]

Similar to the nickel analogue, the mercury complex has four five-membered rings and one nine-membered ring which may explain the difference in bond angles and bond lengths. In the solid state, there are some weak interactions between mercury and oxygen atoms of the perchlorate anions. In addition to that, hydrogen bonding of the type -C···H-, with a bond length of 2.483 Å, is also present between the benzylic hydrogen and the oxygen of the perchlorate anions. Due to these interactions, a chain-like structure is formed.

Table 1. Selected bond lengths (Å) with e.s.d.'s in parentheses for complexes **11**−**16**

Complex **11**			
Ni(1)−N(8)	2.088(3)	Ni(1)−N(8A)	2.088(3)
Ni(1)−N(15)	2.130(5)	Ni(1)−S(10)	2.385(1)
Ni(1)−S(10A)	2.385(1)	Ni(2)−N(23)	2.077(3)
Ni(2)−N(23A)	2.077(3)	Ni(2)−N(30)	2.119(5)
Ni(2)−S(25)	2.379(1)	Ni(2)−S(25A)	2.379(1)
Complex **12**			
Hg(1)−N(9)	2.332(4)	Hg(1)−N(18)	2.363(4)
Hg(1)−N(27)	2.401(4)	Hg(1)−S(20)	2.553(2)
Hg(1)−S(2)	2.577(1)		
Complex **13**			
Cu(1)−N(18)	2.002(4)	Cu(1)−N(9)	2.112(4)
Cu(1)−N(27)	2.132(4)	Cu(1)−S(2)	2.315(2)
Cu(2)−N(48)	2.001(4)	Cu(2)−N(57)	2.112(5)
Cu(2)−N(39)	2.135(5)	Cu(2)−S(32)	2.311(1)
Complex **14**			
Pd(1)−Cl(2)	2.297(2)	Pd(1)−Cl(3)	2.305(2)
Pd(1)−S(2)	2.305(1)	Pd(1)−Cl(1)	2.316(2)
Pd(2)−N(18)	1.988(3)	Pd(2)−S(11)	2.240(1)
Pd(2)−S(20)	2.275(2)	Pd(2)−Cl(4)	2.292(1)
Complex **15**			
Ag(1)−N(27)	2.213(3)	Ag(1)−N(9)	2.398(3)
Ag(1)−N(18)	2.436(4)	Ag(1)−S(11)	2.532(1)
Ag(2)−N(30)	2.245(5)	Ag(2)−S(2)A	2.517(2)
Ag(2)−S(20)	2.545(1)		
Complex **16**			
Ag(1)−N(1)	2.211(4)	Ag(1)−N(2)	2.350(4)
Ag(1)−N(3)	2.383(4)	Ag(1)−S(3)	2.541(1)
Ag(2)−N(1S)	2.286(6)	Ag(2)−S(2)	2.486(1)
Ag(2)−S(1A)	2.551(1)		

Table 2. Selected bond angles (°) with e.s.d.'s in parentheses for complexes **11**−**16**

Complex **11**			
N(8)−Ni(1)−N(8A)	105.72(3)	N(8A)−Ni(1)−N(15)	127.14(9)
N(8)−Ni(1)−N(15)	127.14(9)	N(8A)−Ni(1)−S(10A)	80.24(1)
N(8)−Ni(1)−S(10A)	108.73(10)	N(15)−Ni(1)−S(10A)	82.79(3)
N(8A)−Ni(1)−S(10)	108.73(10)	N(8)−Ni(1)−S(10)	80.24(1)
N(15)−Ni(1)−S(10)	82.79(3)	S(10A)−Ni(1)−S(10)	165.57(6)
N(23)−Ni(2)−N(23B)	106.73(19)	N(23)−Ni(2)−N(30)	126.64(9)
N(23B)−Ni(2)−N(30)	126.64(9)	N(23)−Ni(2)−S(25B)	107.27(9)
N(23B)−Ni(2)−S(25B)	81.25(9)	N(30)−Ni(2)−S(25B)	83.03(3)
N(23)−Ni(2)−S(25)	81.25(9)	N(23B)−Ni(2)−S(25)	107.27(9)
N(30)−Ni(2)−S(25)	81.03(3)	S(25B)−Ni(2)−S(25)	166.06(6)
Complex **12**			
N(9)−Hg(1)−N(18)	110.38(1)	N(9)−Hg(1)−N(27)	125.87(1)
N(18)−Hg(1)−N(27)	123.73(1)	N(9)−Hg(1)−S(20)	120.91(1)
N(18)−Hg(1)−S(20)	74.72(1)	N(27)−Hg(1)−S(20)	77.83(1)
N(9)−Hg(1)−S(2)	74.43(1)	N(18)−Hg(1)−S(2)	121.4(1)
N(27)−Hg(1)−S(2)	76.71(1)	S(20)−Hg(1)−S(2)	154.51(5)
Complex **13**			
N(18)−Cu(1)−N(9)	119.87(2)	N(18)−Cu(1)−N(27)	120.81(2)
N(9)−Cu(1)−N(27)	100.48(2)	N(18)−Cu(1)−S(2)	133.52(1)
N(9)−Cu(1)−S(2)	87.09(1)	N(27)−Cu(1)−S(2)	85.64(1)
N(48)−Cu(2)−N(57)	120.84(2)	N(48)−Cu(2)−N(39)	119.95(2)
N(57)−Cu(2)−N(39)	97.45(2)	N(48)−Cu(2)−S(32)	135.70(2)
N(57)−Cu(2)−S(32)	85.37(2)	N(39)−Cu(2)−S(32)	87.00(2)
Complex **14**			
Cl(2)−Pd(1)−Cl(3)	179.69(5)	Cl(2)−Pd(1)−S(2)	94.14(4)
Cl(3)−Pd(1)−S(2)	86.08(4)	Cl(2)−Pd(1)−Cl(1)	89.94(5)
Cl(3)−Pd(1)−Cl(1)	89.83(5)	S(2)−Pd(1)−Cl(1)	175.09(4)
N(18)−Pd(2)−S(11)	87.58(10)	N(18)−Pd(2)−S(20)	86.49(10)
S(11)−Pd(2)−S(20)	168.39(5)	S(20)−Pd(2)−Cl(4)	95.94(6)
Complex **15**			
N(27)−Ag(1)−N(9)	117.68(1)	N(27)−Ag(1)−N(18)	117.86(1)
N(9)−Ag(1)−N(18)	104.77(1)	N(27)−Ag(1)−S(11)	149.58(8)
N(9)−Ag(1)−S(11)	78.65(9)	N(18)−Ag(1)−S(11)	78.02(9)
N(30)−Ag(2)−S(2)A	119.0(2)	N(30)−Ag(2)−S(20)	111.6(2)
S(2)A−Ag(2)−S(20)	129.08(3)		
Complex **16**			
N(1)−Ag(1)−N(2)	119.27(2)	N(1)−Ag(1)−N(3)	118.32(1)
N(2)−Ag(1)−N(3)	102.02(1)	N(1)−Ag(1)−S(3)	148.30(1)
N(2)−Ag(1)−S(3)	79.08(1)	N(3)−Ag(1)−S(3)	78.16(1)
N(3)−Ag(1)−S(3)	78.16(1)	N(1S)−Ag(2)−S(2)	124.93(2)
N(1S)−Ag(2)−S(1A)	99.50(2)	S(2)−Ag(2)−S(1A)	135.11(4)

Close inspection of the complex crystal structure along the *c*-axis shows that there are six complex cations and six perchlorate anions packed alternately, resulting in a six-membered cyclic ring. The structure forms a hexagonal-shaped space, which may be useful for specific guests.

Structure Description of [Cu(10)(PF$_6$)] (13)

Similar to the nickel complex, the copper complex **13** also has two independent formula units present in one asymmetric unit. The basic molecular geometries are essentially identical, although some insignificant differences in bond lengths and bond angles are observed. The ORTEP diagram of the complex is shown in Figure 4 (left) and Table 1 and 2 provides selected bond lengths and bond angles.

Two exodentate sulfurs are not coordinated to the copper(I) and all attempts to form a coordination polymer containing other metal ions as a bridge between the molecules by using these non-coordinated sulfurs failed. The molecule itself looks like a model of a person, with two exodentate sulfurs as two folded arms, one pyridine as its head and another two pyridines as two legs, as can be easily visualized from the space-filling diagram in Figure 4 (right).

The Cu^{I} ion is encapsulated by the ligand **10** bonding directly to three pyridine nitrogens (N9, N18 and N27 in Cu1 and N39, N48 and N57 in Cu2) and one thioether sulfur (S2 in Cu1 and S32 in Cu2). The remaining two sulfurs are not coordinated to the copper metal and are found at an average non-bonding distance of 4.0 Å. The Cu^{I} ion

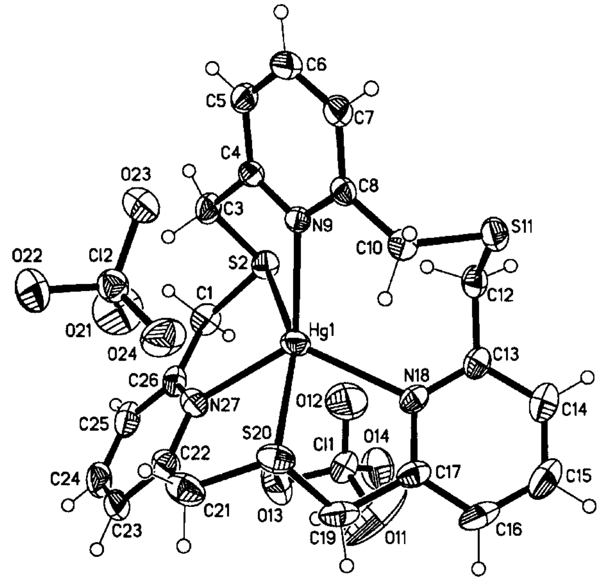

Figure 3. ORTEP drawing of the mercury complex **12**

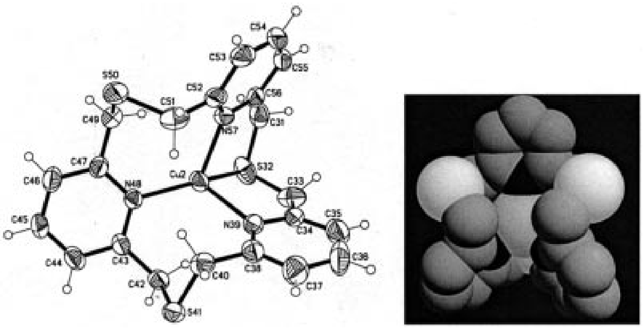

Figure 4. (left) ORTEP drawing of the copper(I) complex **13**; (right) space-filling model of **13** (hydrogen atoms omitted for clarity)

is in a tetrahedral environment with N−Cu−N angles ranging from 119.87(2) to 120.81(2)° for the eight-membered rings and S−Cu−N angles ranging from 85.64(1) to 87.09(1)° for the five-membered rings. The Cu−N and Cu−S distances are in the expected range.[40−43] In the solid-state, the molecules are not discrete but form a network structure through some hydrogen bonding and weak interactions.

Structure Description of [10(PdCl)(PdCl$_3$)] (14)

The X-ray structure of the complex confirms the binuclear complex of formula [(**10**(PdCl)(PdCl$_3$)]. Figure 5 shows an ORTEP diagram of the complex and Table 1 lists selected bond lengths for the metal coordination environment. The two palladium centres are not encapsulated by the ligand but are in a facial coordination. This may be because the cavity of the macrocycle is too small to accommodate two palladium metal ions or to avoid the steric interaction between the metal ions.

Each macrocyclic ligand coordinates to two palladium ions and the structure comprises two different distorted square-planar geometries. In Site A, Pd(1) is coordinated to only one sulfur [Pd−S(2) 2.306 Å] and three chlorine anions (Pd−Cl 2.297, 2.305 and 2.316 Å) and in Site B the metal ion is coordinated to one pyridine nitrogen (Pd−N 1.988 Å), two of the three sulfurs (Pd−S 2.240, 2.275 Å) and one chloride anion (Pd−Cl 2.291 Å). Thus the macrocycle acts simultaneously as a tridentate (NS$_2$) and a monodentate (S) ligand. The remaining two pyridine nitrogens are not coordinated to the palladium metal and are oriented away from it, with non-bonding distances of Pd(2)−N(27) 3.635 Å and Pd(2)−N(9) 3.752 Å. The Pd−N, Pd−S and Pd−Cl distances are within the expected range.[44,45]

The distance between palladium and the non-bonded nitrogens [N(9) and N(27)] is sufficiently large to permit the atoms to be non-interacting, but the nature of the macrocyclic ligand defines a limit for the furthest distance of the non-bonded nitrogens. A value of about 3.6 Å is intermediate between the normal distances for an inner-sphere or coordinated ligand (ca. 2.0 Å) and an outer-sphere or non-coordinated ligand (ca. 4.0 Å). This type of environment may cause unusual and interesting effects in the solution studies.[46] Pd(1) deviates from the mean square plane (S2, Cl1, Cl2, Cl3) by about 0.024 Å, and Pd(2) deviates by about 0.049 Å. It is of interest to note the differences in the Pd−Cl distances found for both coordination sites. Interestingly, the charges of the two palladium centres [Pd(1) and Pd(2)] in each neutral molecule are −1 and +1, respectively, resulting in an inorganic zwitterion.

The intramolecular distance between the two palladium atoms is about 6.9 Å and a short inter-ionic distance of 4.1 Å is observed between palladiums in adjacent dimeric units within the unit cell. These distances are much longer than the 2.751 Å in palladium metal[33] and preclude any metal-metal interaction. When viewed along the *a*-axis, successive layers of the complexes are arranged in an antiparallel fashion [see Figure 6 (left)]. This is due to some hydrogen bonding and other weak interactions[34−37] in the crystal lattice that are listed in Table 1 and 2. In this complex, the three pyridine rings are arranged in a cone-like conformation, as seen in Figure 6 (right). In the crystal packing and along the *c*-axis there are rectangular voids of about 13.3 Å due to these interactions and π-π stacking (3.347 Å to 4.168 Å) of the pyridine rings. Water molecules are also involved in the weak hydrogen-bonding networks.

Structure Description of $[(10)Ag_2(CH_3CN)(PF_6)_2]_\infty$ (15) and $[(10)Ag_2(CH_3CN)(BF_4)_2]_\infty$ (16)

X-ray analysis of complex **15** shows that it is a one-dimensional coordination polymer. The ORTEP diagram of the asymmetric unit of the coordination polymer is shown in Figure 7 (top). One Ag^I resides in the cavity of the macrocycle, coordinated by three N and one S donors; it adopts a distorted tetrahedral geometry with (N,S)−Ag−(S,N)

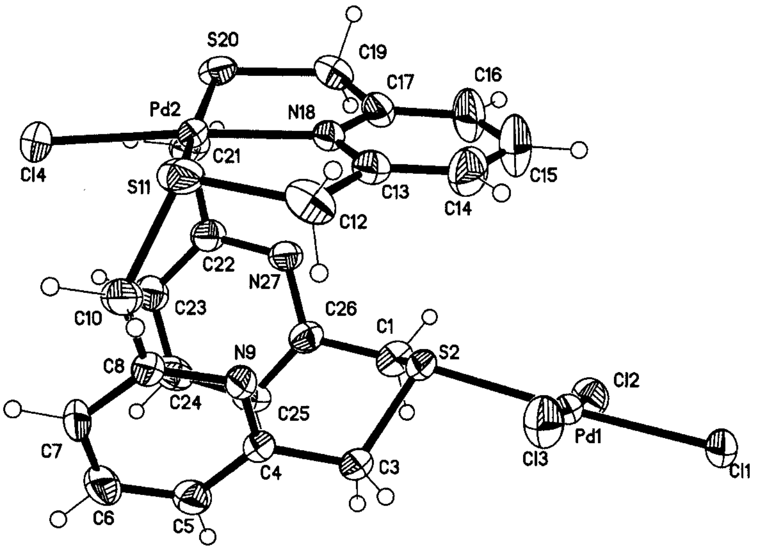

Figure 5. ORTEP diagram of the binuclear palladium complex **14**

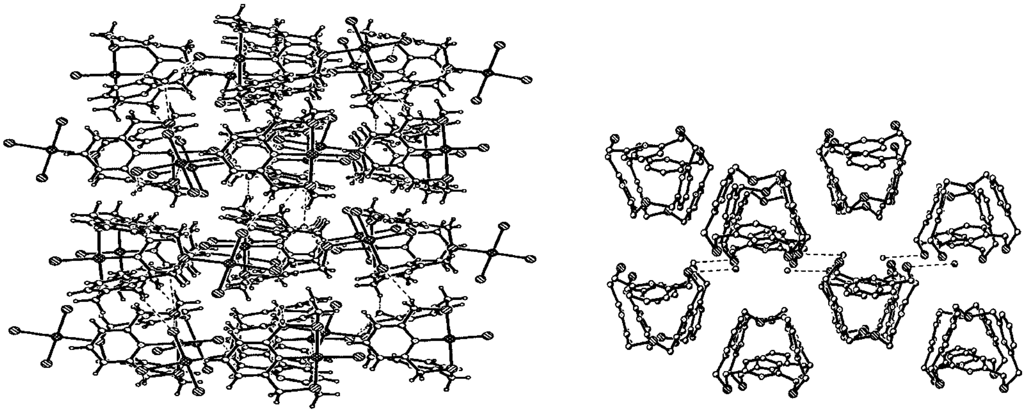

Figure 6. (left) Packing in complex **14** showing the molecules arranged into antiparallel sheets along the *a*-axis; (right) cone conformation in the packing of complex **14**

angles ranging from 78.02(9) to 149.58(8)°, Ag−N bond lengths between 2.213(3) and 2.436(4) Å and an Ag−S distance of 2.532(1) Å. The second Ag^I is coordinated to two S-donors from two different macrocyclic molecules with distances of 2.454(1) and 2.517(1) Å and an acetonitrile solvent molecule($Ag-N-C-CH_3$ 2.245 Å), with a trigonal planar geometry. The silver-acetonitrile nitrogen atom distance of 2.245 Å falls in the range of 2.18−2.33 Å reported previously.[47] Consequently all six donors of each macrocyclic molecule are engaged in coordination. The second Ag^I deviates by about 0.13 Å from the trigonal plane. Two different modes of coordination in a single silver complex are uncommon and the two modes of coordination are shown in Figure 7 (bottom).

Adjacent linear chains are arranged an antiparallel manner, most likely stabilized by the π-π stacking interaction of the pyridine rings. The distance between the π-π pyridine rings is about 3.6 Å, close enough for an interaction. The PF_6 counteranion is situated nicely in the voids between adjacent linear polymer layers and the linear polymers are arranged in a zig-zag fashion along the *c*-axis. Selected bond lengths and bond angles are summarised in Table 1 and 2.

The four-coordinate Ag1 has a long-range interaction with two fluorine atoms of the counterion (Ag1···F 3.379 and 3.562 Å) and hence a pseudo-octahedral geometry is observed. The trigonal planar geometry of the Ag(2) centre is stabilized by interaction of one of the fluorine atoms of

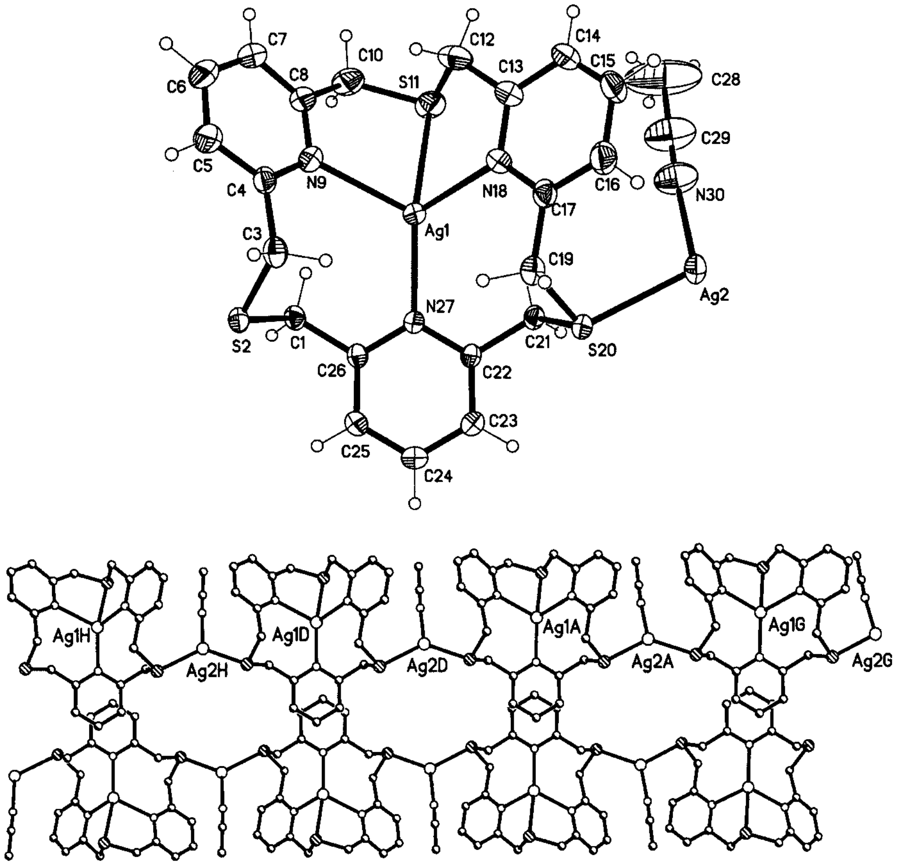

Figure 7. (top) ORTEP diagram of an asymmetric unit of the coordination polymer **15**; (bottom) the two coordination modes of silver in the coordination polymer **15**

the counterion PF_6, at a distance of 2.883 Å, resulting in a pseudo four-coordination. A polymeric disilver complex with two different geometries (tetrahedral and linear) was reported previously[48] with a small macrocycle. To the best of our knowledge, this is the first example of a polymeric complex with a pyridine-containing macrocycle with two different modes of four- and three-coordination. The distance between Ag1 and Ag2 is 5.742 Å and the intermolecular distance between Ag2 and Ag1 of the adjacent macrocycle is about 5.9 Å, which is significantly longer than the sum of their van der Waals radii.

There is no major difference in the X-ray structure when the metal salt is changed from $AgPF_6$ to $AgBF_4$. The complex formed with $AgBF_4$ is also a coordination polymer, with two different coordination modes of silver, with the formula $C_{23}H_{24}Ag_2B_2F_8N_4S_3$. One of the fluorine atoms in BF_4 in the complex **16** is disordered. The bond lengths and bond angles are similar to those of complex **16** listed in Table 1 and 2. The intra- and intermolecular Ag−Ag distances (5.865 Å and 5.657 Å respectively) are different from those in complex **15**. No good quality single crystals could be obtained when $AgNO_3$ was used.

UV/Vis and Redox Properties of the Complexes

The UV/Vis absorption spectrum data of the dinuclear palladium complex is given in the Exp. Sect. The palladium complex is orange and shows an absorption maximum at 374 nm with a further intense absorption band at 272 nm. A peak of this type is absent in most mononuclear complexes and seems to be characteristic of dinuclear palladium complexes, possibly arising from a metal-metal interaction. From previous work the absorption at 272 nm can be assigned to the spin-allowed $4d_{\sigma*} \rightarrow 5p_{\sigma}$ transition.[49] The p_{σ} orbital is a hybrid of the $5p_z$(Pd) and π* (ligand) orbitals. Whether this kind of interaction would lead to some net metal-metal bonding still remains uncertain.

The redox properties of complexes **15** and **16** have been studied by cyclic voltammetry in acetonitrile solution with tetrabutylammonium perchlorate as the supporting electrolyte. Two irreversible reductions are observed at -1.1 and -0.25 V for complex **15** and -1.4 and -0.35 V for complex **16** together with an intense desorption spike at 0 V at a scan rate of 200 $mV \cdot s^{-1}$. Both reductions correspond to a one-electron transfer of Ag^I to Ag^0. No oxidation waves are observed in the cyclic voltammograms up to $+2.0$ V. However, for complex **15** there is an oxidation peak observed at -1.25 V. Similar potential ranges have been reported for related macrocyclic silver complexes.[50]

Extraction Studies

The complexing abilities of the macrocycle **10** with the selected metal cations Ag^I, Cd^{II}, Cu^{II}, Co^{II}, Hg^{II}, Ni^{II}, Pb^{II}

and Zn^{II} were assessed by solvent extraction of the metal chlorides from aqueous solutions into chloroform. The procedure was based on the method used by Kumar et al. and Nishimura et al., in their investigation of mixed nitrogen and sulfur/oxygen-donor cyclophanes.[51,52] The extraction results, presented in Table 3, indicate that the macrocycle has poor selectivity and it extracts all the metals appreciably. Among these metals, macrocycle **10** exhibits a slightly higher preference for Ni^{II}. The observed extraction selectivity order is Ni^{II} > Co^{II} > Zn^{II} > Pb^{II} > Cu^{II} > Cd^{II} > Hg^{II} > Ag^{I}.

Table 3. Relative selectivity in extraction of metal ions by macrocycle **10**

Metal ion	Cd^{II}	Cu^{II}	Co^{II}	Pb^{II}	Hg^{II}	Ni^{II}	Ag^{I}	Zn^{II}
% Extraction	76	77	84	78	69	89	50	83

Conclusions

A hexadentate macrocyclic ligand containing mixed donor atoms, namely [18]aneN_3S_3 (**10**), has been synthesised by a new synthetic route and characterised by analytical and spectroscopic methods. The Ni^{II}, Pd^{II}, Pt^{II}, Cu^{I}, Ag^{I} and Hg^{II} complexes **11−16** of **10** have been prepared and their crystal structures investigated by X-ray crystallography. From the X-ray crystal structures of the complexes, **10** forms mononuclear complexes with nickel, copper and mercury metal ions, a binuclear complex with palladium and coordination polymers with silver. Both nickel and mercury adopt an unusual geometry due to the ligand conformation. The binuclear palladium complex exists as an unusual inorganic zwitterion and a cone conformation of the macrocycle was achieved upon metal ion complexation. The silver complex formed a one-dimensional coordination polymer with two different modes of coordination of silver. Changing the anion of the silver salt does not result in any structural changes in the silver complex. The electronic spectra of the complexes were also investigated. The extraction ability of the macrocycle shows a slightly higher preference for nickel(II). The solid-state packing diagrams in the X-ray structures of the complexes were explained by hydrogen bonding and other weak interactions.

Experimental Section

Materials and Physical Measurements: ^{1}H and ^{13}C NMR spectra were recorded on a Bruker ACF 300 Fourier-transform spectrometer. All chemical shifts are reported in ppm downfield from a tetramethylsilane internal standard. Mass spectra were recorded on a VG Micromass 7035 spectrometer at 70 eV in electron impact mode. Elemental analyses were performed by the Chemical and Molecular Analysis Centre, Department of Chemistry, National University of Singapore. The electronic spectra were recorded using a HP 8452A diode-array UV/Vis spectrophotometer. Cyclic voltammograms were recorded using a single compartment three-electrode cell. A platinum disc of 3 mm in diameter was used as a working electrode. The counter electrode consisted of a platinum wire. All the potentials were measured against the Ag/AgCl couple. An EG&G Princeton Applied Research 273 potentiostat, controlled by M270 software, was used to measure all the electrochemical data. Acetonitrile used for electrochemical studies was triply distilled under nitrogen from calcium hydride and stored over 4-Å molecular sieves. Tetrabutylammonium perchlorate employed as a supporting electrolyte was vacuum dried for 24 h prior to use. All solutions were purged with dry argon for 15 minutes prior to any electrochemical study. The following compounds were prepared according to the literature: 2,6-bis(mercaptomethyl)pyridine (**6**),[53] and 2-bromomethyl-6-hydroxymethylpyridine (**7**).[54]

CAUTION! *Perchlorate salts are potentially explosive and should be handled with care.*

2,6-Bis[(6-hydroxymethyl-2-pyridylmethyl)sulfanylmethyl]pyridine (8): Compound **6** (1.00 g, 5.85 mmol) was added to a solution of sodium ethoxide prepared by dissolving sodium metal (0.27 g, 11.70 mmol) in anhydrous EtOH (200 mL) and the mixture was stirred for 1 h. A solution of compound **7** (2.35 g, 11.70 mmol) in anhydrous EtOH (75 mL) was then added dropwise over 2 h while the reaction mixture was maintained at solvent refluxing temperature. The reaction mixture was allowed to stir for an additional 2 h and cooled to room temperature. The solvent was removed under reduced pressure yielding an orange oil. The crude product was extracted with CH_2Cl_2 and the organic phase was washed with water followed by saturated sodium chloride solution. The solvent was removed and the residue was chromatographed on silica gel (hexane/acetone, 1:1) to give the desired diol **8** as colourless crystals. Yield: 1.95 g (81%); m.p. 83−85 °C. MS: m/z = 413.2 [M$^+$]. ^{1}H NMR ($CDCl_3$): δ = 7.50−7.60 (m, 3 H), 7.20−7.30 (m, 4 H), 7.10 (d, J = 7.62 Hz, 2 H), 4.71 (s, 4 H), 4.30 (br., 2 H), 3.82 (s, 4 H), 3.80 (s, 4 H) ppm. ^{13}C NMR ($CDCl_3$): δ = 158.9, 157.8, 157.3, 137.2, 121.6, 121.3, 118.6, 64.5, 37.2, 37.0 ppm.

2,6-Bis[(6-chloromethyl-2-pyridylmethyl)sulfanylmethyl]pyridine (9) Thionyl chloride (1.04 g, 8.71 mmol, 20% excess) was added slowly with a syringe to a solution of the diol **8** (1.50 g, 3.63 mmol) in CH_2Cl_2 (75 mL) and the mixture was stirred for 6 h at room temperature. A saturated solution of $NaHCO_3$ (50 mL) was added and the mixture was stirred for 1 h. The organic layer was separated and dried. The solvent was removed under reduced pressure yielding brown oil which solidified on standing at 0 °C. Yield: 1.50 g (91%). ^{1}H NMR ($CDCl_3$): δ = 7.62 (m, 2 H), 7.52 (t, J = 7.62 Hz, 1 H), 7.30 (m, 4 H), 7.20 (d, J = 7.62 Hz, 2 H), 4.60 (s, 4 H), 3.76 (s, 4 H), 3.72 (s, 4 H) ppm. ^{13}C NMR: δ = 158.3, 157.8, 156.0, 137.5, 122.5, 121.3, 120.8, 53.3, 37.3, 37.2 ppm. Dichloride **9** decomposes slowly upon standing and was therefore used for the following reaction without further purification.

3,11,19-Trithia[3.3.3]pyridinophane (10): A catalytic amount of NaOH was added to a solution of $Na_2S\cdot 9H_2O$ (0.58 g, 2.40 mmol) in 95% ethanol (250 mL). This was maintained under N_2 at room temperature and a solution of **9** (1.10 g, 2.40 mmol) in EtOH (100 mL) was added dropwise over a period of 6 h. The resulting mixture was then heated to reflux for 6 h. The bulk of the EtOH was removed under reduced pressure and the residue was extracted with chloroform. The organic layer was washed with 0.1 M aqueous NaOH followed by water and dried. The solvent was removed and the residue was recrystallised from acetone to give compound **10**. Yield: 0.68 g (68%); m.p. 158−160 °C. $C_{21}H_{21}N_3S_3$ (411.60): calcd. C 61.28, H 5.15, N 10.21; found C 60.57, H 5.34, N 10.20. MS: m/z = 411.1 [M$^+$]. ^{1}H NMR ($CDCl_3$): δ = 7.59 (t, J = 7.62 Hz, 3 H), 7.27 (d, J = 7.62 Hz, 6 H), 3.81 (s, 12 H) ppm. ^{13}C NMR: δ = 157.7, 137.4, 120.7, 36.7 ppm.

Complex 11: A solution of $Ni(ClO_4)_2 \cdot 6H_2O$ (72.0 mg, 0.18 mmol) in acetonitrile (5 mL) was added to a solution of **10** (40.0 mg, 0.09 mmol) in CH_2Cl_2 (5 mL). The mixture was stirred for 4 h. Slow concentration of the solution gave green crystals of complex **11**. Yield: 53.0 mg (82%). $C_{21}H_{21}N_3NiS_3(ClO_4)_2 \cdot 2H_2O \cdot (CH_2Cl_2)_2$ (960.04): calcd. C 30.03, H 3.25, N 4.38, S 10.02; found C 25.92, H 3.64, N 4.40, S 9.85. FAB-MS: *m*/*z* = 469 [Ni·**10**].

Complex 12: A solution of $Hg(ClO_4)_2 \cdot 6H_2O$ (39.0 mg, 0.10 mmol) in methanol (5 mL) was added to a solution of **10** (20.0 mg, 0.05 mmol) in CH_2Cl_2 (5 mL). A colourless solid precipitated immediately. Diffusion of diethyl ether into a solution of the complex **12** in acetonitrile resulted in isolation of colourless crystals of **12**. Yield: 23.0 mg (60%). $C_{21}H_{21}HgN_3S_3(ClO_4)_2 \cdot 2H_2O$ (847.14): calcd. C 29.77, H 2.95, N 4.96, S 11.36; found C 29.17, H 2.45, N 4.84, S 10.96. FAB-MS: *m*/*z* = 610.9 [Hg·**10**].

Complex 13: $Cu(CH_3CN)_4(PF_6)$ (37.0 mg, 0.10 mmol) was added to a solution of **10** in a mixture of CH_2Cl_2 (5 mL) and methanol (5 mL). The reaction mixture was stirred for 3 h and the solution was concentrated. Slow addition of diethyl ether precipitated light grey crystals of the copper(I) complex **13**. Yield: 29.0 mg (96%); m.p. 136−138 °C (dec.). $C_{21}H_{21}CuF_6N_3PS_3$ (620.13): calcd. C 40.67, H 3.41, N 6.78, S 15.51; found C 42.10, H 3.63, N 7.01, S 15.65. FAB-MS: *m*/*z* = 474.0 [Cu·**10**].

Complex 14: A mixture of **10** (40.0 mg, 0.09 mmol) in CH_2Cl_2 (10 mL) was added to $[PdCl_2(CH_3CN)_2]$ (52.0 mg, 0.18 mmol) in methanol (10 mL) and the mixture was stirred at room temperature for 6 h. On standing dark-orange crystals of complex **14** precipitated from the solution. Yield: 68.0 mg (91%); m.p. 212−215 °C (dec.). $C_{21}H_{21}Cl_4N_3Pd_2S_3 \cdot H_2O$ (784.28): calcd. C 32.16, H 2.95, N 5.35; found C 32.18, H 2.93, N 4.93. FAB-MS: *m*/*z* = 517.0 [Pd·**10**], 552.5 [Pd·**10**·Cl], 624.0 [Pd$_2$·**10**·H], 658.0 [Pd$_2$·**10**·Cl]. UV/Vis: λ_{max} (ε) = 272 (13658), 374 nm (23030 $M^{-1}\,cm^{-1}$).

Complex 15: A solution of $AgNO_3$ (25.0 mg, 0.14 mmol) in acetonitrile (5 mL) was added to a solution of **10** (30.0 mg, 0.07 mmol) in CH_2Cl_2 (5 mL) and the mixture was stirred for 4 h. Addition of a large excess of NH_4PF_6 followed by partial removal of the solvent afforded a white solid. Recrystallisation of this solid from methanol gave a light-sensitive colourless precipitate. Colourless crystals of complex **15** were obtained by diffusion of diethyl ether into a solution of **15** in acetonitrile. Yield: 60.0 mg (86%); m.p. 154−156 °C (dec.). ^1H NMR (CD_3CN): δ = 7.88 (t, *J* = 7.62 Hz, 3 H), 7.47 (d, *J* = 7.62 Hz, 6 H), 4.10 (s, 12 H) ppm. ^{13}C NMR: δ = 157.7, 140.5, 124.8, 38.3 ppm. FAB-MS: *m*/*z* = 518.0 [Ag·**10**], 625.9 [Ag$_2$·**10**·H].

Complex 16: A solution of $AgBF_4$ (15.0 mg, 0.16 mmol) in acetonitrile (5 mL) was added to a solution of **10** (30.0 mg, 0.08 mmol) in CH_2Cl_2 (5 mL) and the mixture was stirred for 4 h. Slow concentration of the solution gave colourless crystals of complex **16**. Yield: 55.0 mg (90%); m.p. 144−146 °C (dec.). ^1H NMR (CD_3CN): δ = 7.87 (t, *J* = 7.62 Hz, 3 H), 7.46 (d, *J* = 7.62 Hz, 6 H), 4.02 (s, 12 H) ppm. ^{13}C NMR: δ = 157.8, 140.4, 124.7, 38.2 ppm. FAB-MS: *m*/*z* = 518.0 [Ag·**10**], 605.0 [Ag·**10**·BF$_4$], 711.9 [Ag$_2$·**10**·BF$_4$·H].

Crystallographic Data Collection and Refinement: Details of the crystal data and refinement of the structures are given in Table 4. Data collection was performed at 293 K using graphite-monochromated Mo-K_α radiation (λ = 0.71073 Å) on a Siemens CCD diffractometer. Structures were solved by Patterson or direct methods. All non-hydrogen atoms were refined anisotropically, except for those of solvent molecules where present. Refinement was done by full-matrix least- squares based on F^2 using SHELXL-93.[55] Hydrogen atoms were introduced at a fixed distance from carbon atoms and their isotropic thermal parameters were based on a riding mode of the parent atoms.

Table 4. Crystallographic data for complexes **11**−**16**

	11	**12**	**13**	**14**	**15**	**16**
Chemical formula	$C_{21}H_{21}Cl_2N_3NiO_8S_3$	$C_{21}H_{21}Cl_2HgN_3O_8S_4$	$C_{21}H_{21}CuF_6N_3PS_3$	$C_{21}H_{23}Cl_4N_3OPd_2S_3$	$C_{23}H_{24}Ag_2F_{12}N_4P_2S_3$	$C_{23}H_{24}Ag_2B_2F_8N_4S_3$
Molecular mass	669.20	811.08	620.10	784.20	958.32	842.00
T (K)	293(2)	293(2)	293(2)	293(2)	293(2)	223(2)
λ (Å)	0.71073	0.71073	0.71073	0.71073	0.71073	0.71073
Crystal system	orthorhombic	monoclinic	triclinic	monoclinic	triclinic	triclinic
Space group	Pnna	$P2_1/c$	$P\bar{1}$	$P2_1/n$	$P\bar{1}$	$P\bar{1}$
a (Å)	16.4967(2)	14.3417(6)	10.6984(9)	12.3992(6)	9.2186(1)	9.0413(2)
b (Å)	22.1884(1)	12.3088(5)	15.4046(1)	14.5148(7)	11.2790(2)	11.021(2)
c (Å)	14.6190(1)	14.8581(6)	16.6414(1)	14.3996(6)	16.9920(2)	14.667(3)
α (°)	90.0	90.0	114.333(2)	90.0	108.726(1)	96.548(4)
β (°)	90.0	92.872(2)	96.459(2)	92.093	94.227(1)	101.866(4)
γ (°)	90.0	90.0	90.262(2)	90.0	92.723(1)	96.730(4)
V (Å^3)	5351.07(8)	2619.59(1)	2479.2(4)	2589.8(2)	1663.95(4)	1405.9(5)
Z	8	4	4	4	2	2
ρ (Mg/cm^3)	1.661	2.057	1.661	2.011	1.913	1.989
μ (mm^{-1})	1.210	6.371	1.260	2.066	1.552	1.693
F (000)	2736	1576	1256	1544	940	828
Crystal size (mm^3)	0.32 × 0.18 × 0.15	0.20 × 0.14 × 0.11	0.15 × 0.12 × 0.10	0.20 × 0.20 × 0.08	0.20 × 0.20 × 0.05	0.68 × 0.50 × 0.14
θ range (°)	1.67 to 27.09	1.42 to 27.49	1.45 to 30.03	2.13 to 30.92	1.91 to 28.34	1.88 to 25.00
Index ranges	$-20 \le h \le 16$	$-18 \le h \le 18$	$-15 \le h \le 15$	$-16 \le h \le 17$	$-11 \le h \le 12$	$-10 \le h \le 10$
	$-28 \le k \le 26$	$-15 \le k \le 10$	$-21 \le k \le 21$	$-20 \le k \le 20$	$-14 \le k \le 15$	$-13 \le k \le 13$
	$-18 \le l \le 18$	$-17 \le l \le 19$	$-23 \le l \le 23$	$-10 \le l \le 19$	$-22 \le l \le 22$	$-17 \le l \le 17$
Reflections collected	30061	17925	28159	21186	15423	11550
Independent reflections	5767 *R*(int) = 0.0559	5894 *R*(int) = 0.0495	13929 *R*(int) = 0.0367	7547 *R*(int) = 0.0273	7885 *R*(int) = 0.0177	4953 v(int) = 0.0699
Max and min transmission	0.942 and 0.658	0.694 and 0.496	0.928 and 0.692	0.928 and 0.701	0.928 and 0.770	0.675 and 0.418
Data/restraints/parameters	5766/0/347	5894/0/343	13929/0/631	7547/0/304	7883/27/451	4953/108/392
Goodness of fit on F^2	1.061	0.758	0.958	0.982	1.042	1.172
Final *R* indices	*R*1 = 0.0539	*R*1 = 0.0374	*R*1 = 0.0807	*R*1 = 0.0460	*R*1 = 0.0422	*R*1 = 0.0559
[$I > 2\sigma(I)$]	*wR*2 = 0.1274	*wR*2 = 0.0568	*wR*2 = 0.2339	*wR*2 = 0.1157	*wR*2 = 0.1154	*wR*2 = 0.1482
R indices	*R*1 = 0.0903	*R*1 = 0.0750	*R*1 = 0.1490	*R*1 = 0.0668	*R*1 = 0.0568	*R*1 = 0.0586
(all data)	*wR*2 = 0.1522	*wR*2 = 0.0624	*wR*2 = 0.2582	*wR*2 = 0.1239	*wR*2 = 0.1263	*wR*2 = 0.1512
Largest difference peak and hole (e·Å^{-3})	0.814 and −0.556	1.378 and −0.734	0.864 and −0.483	1.301 and −1.119	1.057 and −0.583	0.957 and −0.786

Acknowledgments

This work was supported by the National University of Singapore, Singapore (NUS) with grant no. R-143-000-026-112. M.V. thanks the NUS for a research scholarship. Assistance from the technical staff of the Department of Chemistry, NUS, is gratefully acknowledged.

[1] A. J. Blake, N. R. Champness, P. Hubberstey, W. S. Li, M. A. Withersby, M. Schröder, *Coord. Chem. Rev.* **1999**, *183*, 117–138.

[2] P. J. Stang, B. Olenyuk, *Acc. Chem. Res.* **1997**, *30*, 502–518.

[3] N. R. Champness, M. Schröder, *Curr. Opin. Solid State Mater. Sci.* **1998**, *3*, 419–424.

[4] O. M. Yaghi, H. Li, C. Davis, D. Richardson, T. L. Groy, *Acc. Chem. Res.* **1998**, *31*, 474–484.

[5] G. R. Desiraju, *Angew. Chem. Int. Ed. Engl.* **1995**, *34*, 2311–2317.

[6] G. R. Desiraju, *Crystal Engineering: Design of Organic Solids*, Elsevier, Amsterdam, **1989**.

[7] H. W. Yin, L. M. Tran, E. E. Pullen, R. Daniel, M. L. Louise, E. C. Thomas, A. L. Rheingold, *Inorg. Chem.* **1999**, *38*, 6234–6239.

[8] S. Sailaja, M. V. Rajasekaran, *Inorg. Chem.* **2001**, *39*, 4586–4590.

[9] L. Fabbrizi, A. Poggi, *Transition Metals in Supramolecular Chemistry*, Kluwer Academic Publishers: Dordrecht, The Netherlands, **1994**.

[10] R. Thaimattam, F. Xue, J. A. R. P. Sarma, T. C. W. Mak, G. R. Desiraju, *J. Am. Chem. Soc.* **2001**, *123*, 4432–4445.

[11] M. Hong, W. Su, R. Cao, W. Zhang, J. Lu, *Inorg. Chem.* **1999**, *38*, 600–602 and references therein.

[12] S. Yusaku, K. S. Takayoshi, M. Masahiko, M. Munakata, *J. Chem. Soc., Dalton Trans.* **1999**, 2737–2741.

[13] G. R. Newkome, J. D. Sauer, J. M. Roper, D. C. Hager, *Chem. Rev.* **1977**, *77*, 513–597.

[14] F. H. Fry, P. Jensen, C. M. Kepert, L. Spiccia, *Inorg. Chem.* **2003**, *42*, 5637–5644 and references therein.

[15] S. A. Li, J. Xia, D. X. Yang, Y. Xu, D. F. Li, M. F. Wu, W. X. Tang, *Inorg. Chem.* **2002**, *41*, 1807–1815 and references therein.

[16] A. J. Blake, W. S. Li, V. Lippolis, M. Schröder, *Chem. Commun.* **1997**, 1943–1944 and references therein.

[17] A. J. Blake, D. Collison, R. O. Gould, G. Reid, M. Schröder, *J. Chem. Soc., Dalton Trans.* **1993**, 521–531.

[18] A. J. Blake, M. Schröder, *Adv. Inorg. Chem.* **1990**, *35*, 1–80.

[19] A. J. Blake, N. R. Champness, S. M. Howdle, P. B. Webb, *Inorg. Chem.* **2000**, *39*, 1035–1038 and references therein.

[20] P. J. Blower, J. A. Clarkson, S. C. Rawle, J. R. Hartman, R. E. Wolf Jr., R. Yagbasan, S. G. Bott, S. R. Cooper, *Inorg. Chem.* **1989**, *28*, 4040–4046.

[21] S. C. Rawle, S. R. Cooper, *Struct. Bonding* **1990**, *72*, 1–72.

[22] L. R. Hanton, C. Richardson, W. T. Robinson, J. M. Turnbull, *Chem. Commun.* **2000**, 2465–2466 and references therein.

[23] M. Munakata, L. P. Wu, M. Yamamoto, T. Kuroda-Sowa, M. Maekawa, *J. Chem. Soc., Dalton Trans.* **1995**, 3215–3220.

[24] R. Alberto, D. Angst, U. Abram, K. Ortner, T. A. Kaden, P. August, *Chem. Commun.* **1999**, 1513–1514 and references therein.

[25] F. Vöegtle, F. Ley, *Chem. Ber.* **1983**, *116*, 3000–3002.

[26] S. J. Loeb, K. D. L. Smith, *Inorg. Chem.* **1993**, *32*, 1297–1300.

[27] J. Buter, R. M. Kellogg, *J. Org. Chem.* **1981**, 4481–4485.

[28] J. Buter, R. M. Kellogg, *Org. Synth.* **1987**, *65*, 150–158.

[29] A. W. Addision, T. N. Rao, J. Reedijk, J. van Rijn, G. C. Verschoor, *J. Chem. Soc., Dalton Trans.* **1984**, 1349–1356.

[30] L. Sacconi, F. Mani, A. Bencini, in *Comprehensive Coordination Chemistry* (Eds.: G. Wilkinsen, R. D. Gillard, J. A. McCleverty), Pergamon Press: New York, **1987**, 5, 86.

[31] J. G. Gilbert, A. W. Addison, R. J. Butcher, *Inorg. Chim. Acta* **2000**, *308*, 22–30.

[32] R. Morassi, I. Bertini, L. Sacconi, *Coord. Chem. Rev.* **1973**, *11*, 343–402.

[33] P. A. Duckworth, F. S. Stephens, K. P. Wainwright, K. D. V. Veerasuria, S. B. N. Wild, *Inorg. Chem.* **1989**, *28*, 4531–4535.

[34] G. R. Desiraju, *Acc. Chem. Res.* **1996**, *29*, 441–449.

[35] P. G. Jones, B. Aherns, *Chem. Commun.* **1998**, 2307–2308.

[36] T. Steiner, *Chem. Commun.* **1997**, 727–728.

[37] T. C. Deivaraj, J. J. Vittal, *J. Chem. Soc., Dalton Trans.* **2001**, 322–328.

[38] A. McAuley, T. W. Whitecombe, M. J. Zaworotko, *Inorg. Chem.* **1991**, *30*, 3513–3520.

[39] D. C. Bebout, A. E. DeLanoy, D. E. Ehmann, M. E. Kastner, D. A. Parrish, R. J. Butcher, *Inorg. Chem.* **1998**, *37*, 2952–2959.

[40] A. M. W. C. Thompson, I. Blandfors, H. Redfearn, J. C. Jeffery, M. D. Ward, *J. Chem. Soc., Dalton Trans.* **1997**, 2661–2666.

[41] B. D. Groot, S. J. Loeb, *Inorg. Chem.* **1989**, *28*, 3573–3578.

[42] B. D. Groot, G. R. Giesbrecht, S. J. Loeb, G. K. H. Shimizu, *Inorg. Chem.* **1991**, *30*, 177–182.

[43] F. R. Fronczek, P. J. Schilling, S. F. Watkins, V. K. Majestic, G. R. Newcomb, *Inorg. Chim. Acta* **1996**, *246*, 119–123 and references therein.

[44] K. Wieghardt, H. J. Kuppers, E. Raabe, C. Kruger, *Angew. Chem. Int. Ed. Engl.* **1986**, *25*, 1136–1138.

[45] R. A. Newman, D. S. Martin, R. F. Dallinger, W. H. Woodruff, A. E. Stiegman, C. M. Che, W. P. Schaefer, V. M. Miskowski, H. B. Gray, *Inorg. Chem.* **1991**, *30*, 4647–4654.

[46] G. Hunter, A. McAuley, T. W. Whitecombe, *Inorg. Chem.* **1988**, *27*, 2634–2639.

[47] H. Adams, N. A. Bailey, P. Bertrand, S. R. Collinson, D. E. Fenton, S. J. Kitchen, *Inorg. Chim. Acta* **1996**, *250*, 139–148.

[48] H. J. Drexler, M. Grotjahn, E. Kleinpeter, H. J. Holdt, *Inorg. Chim. Acta* **1999**, *285*, 305–308.

[49] H. K. Yip, T. F. Lai, C. M. Che, *J. Chem. Soc., Dalton Trans.* **1991**, 1639–1641.

[50] A. J. Blake, W. S. Li, V. Lippolis, A. Taylor, M. Schröder, *J. Chem. Soc., Dalton Trans.* **1998**, 2931–2938 and references therein.

[51] S. Kumar, M. S. Hundal, G. Hundal, P. Singh, V. Bhalla, H. Singh, *J. Chem. Soc., Perkin Trans. 2* **1998**, 925–932.

[52] S. Inokuma, K. Kimura, T. Funaki, J. Nishimura, *Heterocycles* **2001**, *54*, 123–130.

[53] E. C. Constable, A. C. King, P. R. Raithby, *Polyhedron* **1998**, *17*, 4275–4289.

[54] M. Newcomb, J. M. Timko, D. M. Walba, D. J. Cram, *J. Am. Chem. Soc.* **1977**, *99*, 6392–6398.

[55] G. M. Sheldrick, SHELXL 93, *Program for Crystal Structure Refinement*, University of Göttingen, **1993**.

Received November 12, 2003
Early View Article
Published Online April 1, 2004